Central Lancashire Online Knowledge (CLoK)

Title	Analysis of Multi-Temporal Shoreline Changes Due to a Harbor Using Remote Sensing Data and GIS Techniques
Type	Article
URL	https://clok.uclan.ac.uk/46750/
DOI	https://doi.org/10.3390/su15097651
Date	2023
Citation	Zoysa, Sanjana, Basnayake, Vindhya, Samarasinghe, Jayanga T., Gunathilake, Miyuru B., Kantamaneni, Komali, Muttil, Nitin, Pawar, Uttam and Rathnayake, Upaka (2023) Analysis of Multi-Temporal Shoreline Changes Due to a Harbor Using Remote Sensing Data and GIS Techniques. Sustainability, 15 (9).
Creators	Zoysa, Sanjana, Basnayake, Vindhya, Samarasinghe, Jayanga T., Gunathilake, Miyuru B., Kantamaneni, Komali, Muttil, Nitin, Pawar, Uttam and Rathnayake, Upaka

It is advisable to refer to the publisher's version if you intend to cite from the work.
https://doi.org/10.3390/su15097651

For information about Research at UCLan please go to http://www.uclan.ac.uk/research/

Article

Analysis of Multi-Temporal Shoreline Changes Due to a Harbor Using Remote Sensing Data and GIS Techniques

Sanjana Zoysa [1], Vindhya Basnayake [2], Jayanga T. Samarasinghe [3], Miyuru B. Gunathilake [4,5],
Komali Kantamaneni [6], Nitin Muttil [7,8], Uttam Pawar [9] and Upaka Rathnayake [10,*]

1   Department of Civil Engineering, Faculty of Engineering, Sri Lanka Institute of Information Technology,
    Malabe 10115, Sri Lanka
2   Department of Water Engineering and Management, University of Twente,
    7522 NB Enschede, The Netherlands
3   Department of Earth Environmental and Resource Sciences, University of Texas, El Paso, TX 79968, USA
4   Hydrology and Aquatic Environment, Environment and Natural Resources, Norwegian Institute of
    Bioeconomy and Research, 1433 Ås, Norway
5   Water, Energy, and Environmental Engineering Research Unit, Faculty of Technology, University of Oulu,
    P.O. Box 8000, FI-90014 Oulu, Finland
6   School of Engineering, University of Central Lancashire, Preston PR1 2HE, UK
7   Institute for Sustainable Industries & Liveable Cities, Victoria University, P.O. Box 14428,
    Melbourne, VIC 8001, Australia
8   College of Sport, Health and Engineering, Victoria University, P.O. Box 14428, Melbourne, VIC 8001, Australia
9   Department of Geography, HPT Arts and RYK Science College, Nashik 422005, Maharashtra, India
10 Department of Civil Engineering and Construction, Faculty of Engineering and Design,
    Atlantic Technological University, F91 YW50 Sligo, Ireland
*   Correspondence: upaka.rathnayake@atu.ie

Abstract: Coastal landforms are continuously shaped by natural and human-induced forces, exacerbating the associated coastal hazards and risks. Changes in the shoreline are a critical concern for sustainable coastal zone management. However, a limited amount of research has been carried out on the coastal belt of Sri Lanka. Thus, this study investigates the spatiotemporal evolution of the shoreline dynamics on the Oluvil coastline in the Ampara district in Sri Lanka for a two-decade period from 1991 to 2021, where the economically significant Oluvil Harbor exists by utilizing remote sensing and geographic information system (GIS) techniques. Shorelines for each year were delineated using Landsat 5 Thematic Mapper (TM), Landsat 7 Enhanced Thematic Mapper Plus (ETM+), and Landsat 8 Operational Land Imager images. The Normalized Difference Water Index (NDWI) was applied as a spectral value index approach to differentiate land masses from water bodies. Subsequently, the Digital Shoreline Analysis System (DSAS) tool was used to assess shoreline changes, including Shoreline Change Envelope (SCE), Net Shoreline Movement (NSM), End Point Rate (EPR), and Linear Regression Rate (LRR). The results reveal that the Oluvil coast has undergone both accretion and erosion over the years, primarily due to harbor construction. The highest SCE values were calculated within the Oluvil harbor region, reaching 523.8 m. The highest NSM ranges were recorded as −317.1 to −81.3 m in the Oluvil area and 156.3–317.5 m in the harbor and its closest point in the southern direction. The maximum rate of EPR was observed to range from 3 m/year to 10.7 m/year towards the south of the harbor, and from −10.7 m/year to −3.0 m/year towards the north of the harbor. The results of the LRR analysis revealed that the rates of erosion anomaly range from −3 m/year to −10 m/year towards the north of the harbor, while the beach advances at a rate of 3 m/year to 14.3 m/year towards the south of the harbor. The study area has undergone erosion of 40 ha and accretion of 84.44 ha. These findings can serve as valuable input data for sustainable coastal zone management along the Oluvil coast in Sri Lanka, safeguarding the coastal habitats by mitigating further anthropogenic vulnerabilities.

Keywords: digital shoreline analysis system (DSAS); Landsat; net shoreline movement (NSM); normalized difference water index (NDWI); Oluvil harbor; shoreline change envelope (SCE)

1. Introduction

Coastal environments are found in the dynamic interface between the Earth's three main natural systems of land, sea, and atmosphere. These areas are characterized by their dynamic nature, as they are constantly influenced by the interaction of these three systems [1]. Despite covering only a small fraction (<15%) of the total land area of the earth, coastlines are among the most densely populated areas globally, home to 60% of the people in the world [2,3], with many coastal cities and towns relying on the ocean for their livelihoods [4]. However, over the last three decades, the magnitude and frequency of natural processes, for instance, sea level rise and storms, have increased as a result of climate change, while at the same time, the pressures of industrial activities, urbanization, and tourism have put a strain on coastal areas [5,6]. For instance, according to a study conducted by Palamakumbure et al. [7] on the southern and southwestern coasts of Sri Lanka, the sea level has been increasing at a rate of 0.288 ± 0.118 mm per month. It is predicted that in the next 50 years, the sea level will rise by approximately 0.1 m to 0.2 m, resulting in an inundation of less than 1.8 m from the current sea level towards the inland. Additionally, the study has suggested that in the next 200 years, the sea level is expected to rise by about 0.7 m, resulting in an inundation of 3.5 m to 15.0 m from the current sea level towards the inland. The process of shoreline change is a common issue that arises in coastal environments. Shorelines demarcate the transition zone between land and sea and are home to diverse habitats such as sandy beaches, rocky cliffs, tidal flats, and estuaries [8]. These habitats provide crucial ecosystem services such as erosion control, nutrient cycling, and habitat for fish and wildlife [9]. Hence, the study of shoreline changes is a crucial aspect of the management and sustainability of coastal zones.

The shoreline changes occur primarily due to coastal erosion, which is caused by a variety of factors that can be broadly categorized into two types: erosion due to natural causes and erosion due to human interventions. The coastal belt of southeastern Sri Lanka is confined to a slender land strip measuring approximately 1.5 km in width. The beach is frequently plagued by natural disasters such as monsoons, tropical storms, surges, depressions, flash floods, and tsunamis. For example, Lanka et al. [10] reported that the Batticaloa cyclone of 1978, considered one of the most disastrous cyclones to have hit Sri Lanka, resulted in widespread destruction in the study area as a result of the heavy rain and storm surges it caused. The Oluvil region was severely impacted by the 2004 tsunami, which was another catastrophic disaster to strike the area [11–13]. Additionally, the area is susceptible to storm surges resulting from frequent depressions within the Bay of Bengal [14]. The vulnerability of shorelines due to these kinds of various natural phenomena such as storm-induced erosion, sea level rise, oceanic over-wash, longshore sediment transport, and flooding has been extensively studied worldwide [15–18]. In addition to these factors, shoreline erosion is sometimes exacerbated by human interventions such as modifications and constructions along the shoreline. Based on Dean and Galvin [19], the increase in sea level leads to a rate of long-term shoreline recession of 1 to 3 ft/year in most areas. Nevertheless, localized erosion rates of 10 to 20 ft/year can occur in the regions with high rates of longshore transport, due to shoreline construction, which is significantly higher than the average rate of 1 to 3 ft/year. Aladwani [20] reported that the extensive construction project and associated infrastructure in Al-Khiran, Kuwait, which was extended to the sea, resulted in a decrease in the rate of both accretion and erosion along the coast. Moreover, according to Abualtayef et al. [21], the accretion rate at the Mediterranean coast of Gaza increased drastically following the completion of a harbor construction. According to the figures from the Coast Conservation and Coastal Resource Management Department (CCCRMD), Sri Lanka, LKR 1.52 billion was spent on coastal erosion management from 1985 to 1999, and this amount increased to LKR 3 billion from 2001 to 2007 under the auspicious ADB-funded project on coastal resource management. Additionally, LKR 2 billion was expended for sand replenishment and coastal protection in the western, southern, and northwestern regions [22]. Hence, monitoring shoreline changes is crucial for both environmental and socio-economic reasons, given the significant funds allocated for coastal conservation in

recent decades. The measurement of shoreline changes has often been determined through various techniques including field surveys, tracing of shorelines from topographic sheets, and aerial photographs analyzed with different methods [23,24]. The shoreline's temporal variability, the accuracy of shoreline measurement, the number of data points, the non-uniform time interval between shoreline measurements, the chosen analytical technique, and the overall time period of shoreline data acquisition are all important considerations when evaluating the reliability of these methods. For example, aerial photography provides highly detailed images of shorelines but only captures the shoreline's position at the moment of acquisition [25–27]. Airborne LiDAR (Light Detection and Ranging) is another increasingly popular high-resolution satellite imagery method [28–32]; however, its spatial coverage is limited to certain areas including Australia, Canada, USA, Japan, Scotland, and New Zealand [28]. Other survey methods such as Synthetic Aperture Radar (SAR) and WorldView 2 also have been used to determine shoreline positions in some research [33,34]. Despite their usefulness, the above survey methods can be particularly challenging and resource intensive, especially when considering extensive study areas. This is due to the unavailability of free data, time, and cost involved in conducting these surveys, as noted by Aladwani. [20] and Maiti and Bhattacharya., [35]. In recent years, satellite imagery-based remote sensing techniques have become a popular method for shoreline monitoring due to their ability to cover large areas in a timely manner, being less resource-intensive, and being more efficient [36–40]. In addition, the easy and free accessibility of satellite imagery has led to the widespread adoption of remote sensing and GIS techniques for assessing and monitoring shoreline positions [41]. Landsat satellite images, for example, provide an excellent source of information on shoreline changes, offering synoptic and repeatable data over large spatial and temporal scales [42]. They are available through a series of sensors including the Thematic Mapper (TM), Multispectral Scanner System (MSS), Enhanced Thematic Mapper Plus (ETM+), and Operational Land Imager (OLI). Despite the free accessible ample image collection that allows for the development of long-term analyses lasting between 10 and 30 years, the primary limitation of the Landsat project is its spatial resolution of 30 m [43,44]. The TM, ETM+, and OLI sensors currently provide medium spatial resolution (30 m) with 8 days of combined repetitive coverage. The TM, ETM+, and OLI sensors offer a medium spatial resolution of 30 m and combined repetitive coverage of 8 days [45–47]. The integration of Landsat images with GIS techniques and shoreline analysis tools such as the Digital Shoreline Analysis System (DSAS) has been broadly used to analyze and monitor shoreline changes in many parts of the world including the Mediterranean coast [45], the Gulf of Mannar [48], and the Eastern Coast of Algeria [49]. This tool provides an automated method for the calculation of rate-of-change statistics and allows for the assessment of their robustness [35,50].

A variety of shoreline indicators have been documented in the scientific literature [32,51]. Examples include visually noticeable indicators such as the previous high-tide line or the dry/wet boundary, as well as tidal datum-based indicators such as mean high water (MHW) or mean sea level and indicators derived from the approach taken for shoreline extraction using image analysis. Therefore, defining the shoreline can present a challenge, given the range of indicators cited in the literature, specifically in macro-tidal coasts. In micro-tidal zones, the water/land line is typically used as the shoreline indicator, while the dry/wet sand line is often employed in macro-tidal areas [43]. Hence, for the present study, we have chosen to use the water/land line as the shoreline indicator, given that the Sri Lankan coast exhibits micro-tidal ranges.

Over the past few decades, various image processing techniques have been developed for extracting water features from satellite data. These include high water-line (HWL) visual interpretation [52–54], edge detection [55] (Liu and Jezek, 2004), water indexes [37,39], segmentation and single-band threshold [38,56], multi-band methods combining different reflective bands [57], and segmentation based on local spectral histogram and level set method [58]. Some of these techniques involve manual detection, while others allow for automatic image processing. The latter is particularly important for long-term studies, as

it reduces human errors and improves standardization and efficiency [55,59]. The main reason for this is that the manual delineation of the shoreline by remote sensing imagery is often subjective. Therefore, manual derivation of shorelines over a prolonged period can be challenging, and most of the literature implies that the accuracy of the map is directly related to the user's experience [38,44,55]. Therefore, numerous algorithms have been developed worldwide for detecting and separating waterlines in remote sensing imagery. These algorithms leverage various indices such as the Automated Water Extraction Index (AWEI), Normalized Difference Water Index (NDWI), Modified Normalized Difference Water Index (MNDWI), and Normalized Difference Vegetation Index (NDVI) [47,60,61].

Sri Lanka is an island nation located in the southwest of the Bay of Bengal in the Indian Ocean at the southern tip of India. The country has a diverse coastline that spans approximately 1700 km and features various geomorphological formations including bays, lagoons, and islets [62]. In recent years, numerous studies have been undertaken to evaluate the extent and impact of coastal erosion along Sri Lanka's southern and western coasts [63–65]. However, less attention has been paid to understanding the coastal transformations along the island's eastern coast. The eastern coastal belt of Sri Lanka is home to numerous critical features including harbors such as Oluvil, Trincomalee, and Hambantota as well as urbanized areas and tourist destinations such as Nilaveli, Pasikuda, and Arugambay, important conservation sites such as Yala and Kumana national parks, and high-quality mineral reserves such as Pulmoddai, Verugal, and Kokkilai [66]. As a result, this area holds immense significance both environmentally and in terms of development for the country. Furthermore, after the end of the civil war in 2009, the east coast of Sri Lanka experienced rapid urbanization and the implementation of various development projects such as Oluvil harbor. The Oluvil region in the Ampara district of Sri Lanka has been experiencing significant erosion in the coastline over the past several years [67]. The construction of the Oluvil harbor is widely believed to be the reason for this erosion by the local community. Many people question the construction of this harbor due to the issues that they are facing now. The harbor may not be efficient, at least in the context of environmental aspects. It could be due to a combination of administrative errors, business pressures, engineering incompetence, and political pressure in the construction of the harbor. There have been several studies in various parts of the world on the impact of harbor construction on the coastal zone, and their findings have also shown that harbor construction can cause significant changes in the shoreline position and shape [21,68,69]. Even though there are many studies available on east coastline variation, to the authors' knowledge, no study has been completed that investigates the Oluvil coastline variation in Sri Lanka over 20 years with an adequate amount of data. Given the importance, this study aims to focus on the changes in a 9 km stretch of the coastal belt near the Oluvil harbor. It is essential to examine the rate of change of shorelines before commencing and after completing the construction of the harbor to accurately evaluate its impact. Calculating shoreline changes in the Oluvil coastal belt is essential; hence, this study has three key objectives: (1) to identify the most impacted coastal stretches by calculating the shoreline change (eroded and accreted areas); (2) to compare the rate of shoreline change before and after the completion of giant development projects such as the Oluvil harbor; (3) to calculate the amount of shoreline degradation or progradation that has occurred in the study region over the course of the study period.

2. Study Area

Sri Lanka is located in the Indian Ocean south of India. The island has a densely populated coastline of approximately 1680 km including 82 lagoons, and is home to 14.6 million people. Among these, the eastern coastline is rapidly developing, populous, and one of the busiest regions in the country [70]. Oluvil Harbor is the first major port infrastructure developed on the eastern coastline of Sri Lanka. The study area of Oluvil harbor is located facing the Bay of Bengal, with an eastern latitude of 81°51′55″ and northern longitude of 7°16′34″ (Refer to Figure 1). The coastline stretches for approximately 16 km, spanning from

Nintavur in the north to Addalaichenai in the south, with interruptions by the Kaliodai and Periyappalam rivers (Refer to Figure 1).
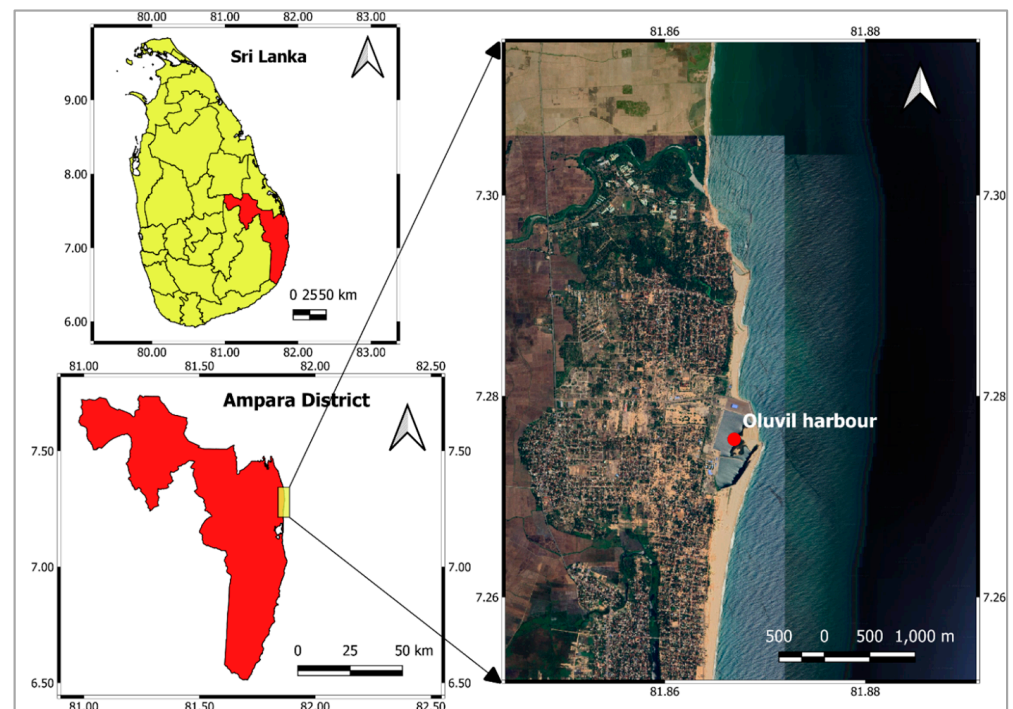
Figure 1. Location map of the study area—Oluvil Harbor, Sri Lanka.

The Oluvil beach is configured with gentle fine sand. Bays, headlands, long straight sandy beaches, and deltas comprise the primary landforms that characterize the geomorphology of the east coast. Generally, the tidal range around a coast has been classified as micro-tidal—when the tidal range is lower than 2 m; meso-tidal—when the tidal range is between 2–4 m; and macro-tidal—when the tidal range is higher than 4 m [71] (Short, 1991). The tide around Sri Lanka is mixed semidiurnally with a spring tidal range of between 0.40 and 0.60 m showing a micro-tidal range. Hence, variability of the tidal range on the Sri Lankan coast is comparably lower but slightly higher on the east and west coasts (0.44 m) than in other regions of the country [72]. Therefore, according to Frigaard and Margheritini [73] and Nijamir et al. [67], tidal fluctuation has a lower impact on the coast in the study area and causes slight seasonal modifications in the shorelines. The seasonal range of sea level around the coast of Sri Lanka is 20 cm to 30 cm, and it has been reported that the wave heights range from 0.5 m to 2.0 m on the coast of the study area [73,74]. The dynamics of the monsoonal wind cause coastal morphological changes. The coastal area of Sri Lanka receives two monsoons: southwest (SWM) from December to February and northeast (NEM) from May to September. The maximum water level is observed in December–January, while the minimum sea water level is observed in August–September, due to the influence of monsoonal winds. During these periods, erosion increases on the coast due to the increasing inundation for the maximum sea water level, while sedimentation occurs along the study area for the minimum water level. Longshore sediment transport from south to north is also triggered by waves from the southern direction, resulting in sedimentation in the port entrance and anomalous erosion and accretion in the north and south, respectively [75]. Additionally, waves from northerly directions also create longshore sediment transport from south to north, resulting in accretion in the port entrance and erosion in the southward direction of the port. During the NEM, waves typically approach the shore from directions between 110° and 130°, with an average significant wave height of 0.29 m in the swell, while during the SEM, waves usually arrive from directions between 100° and 140°, with a mean wave height of 0.28 m in the swell. Moreover, during the NEM, waves can also come

from directions between 30° and 100°, with an average wave height of 0.89 m in the sea; similarly, during the SEM, waves may approach from directions between 110° and 150°, with a mean wave height of 0.16 m in the sea [76,77]. There is currently a lack of reliable data regarding the measured rates of sediment transport in Oluvil. However, a recent numerical modeling study conducted at Oluvil harbor estimated that the net longshore sediment rate is approximately 350,000 m^3/per year [76].

3. Materials and Methodology

3.1. Data Acquisition

A time series of remote sensing images were employed to analyze shoreline changes along the Oluvil coastline. The primary data source consisted of Landsat 5-Thematic Mapper (TM), Landsat 7-Enhanced Thematic Mapper Plus (ETM+), and Landsat 8-Operational Land Imager (OLI) images with a 30 m spatial resolution. These images were obtained free of charge from the United States Geological Survey (USGS) Earth Explorer portal (https://earthexplorer.usgs.gov/) (accessed on 23 November 2022) and were selected based on low or no cloud coverage. Due to the cloud coverage, and limited availability of suitable images, 24 images captured between 1991 and 2021 were utilized in the present study and the details of the employed Landsat image products are mentioned in Table 1. To supplement our analysis, we also incorporated satellite images from Google Earth Pro software for each period between 1991 and 2021, which enabled us to observe and compare changes while delineating the shoreline. Lakmali et al. [64] reported that significant erosion occurs along the southwestern coastline of Sri Lanka during the southwestern monsoon period, but the areas mostly recover during the fair-weather northeastern monsoon conditions. Therefore, severe long-term erosion conditions do not persist in the western, southwestern, and northwestern coasts. However, some isolated locations along the northeastern and eastern coastline experience considerable erosion. Therefore, to avoid the seasonal impact on the results, the authors only considered satellite images taken during the southwestern monsoon period on the image availability (Refer to Table 1).

Table 1. Details of the Landsat Image Data Used (Source—The United States Geological Survey, 2022, https://www.usgs.gov/ (accessed on 23 November 2022).

| Image Source	Bands	Wavelength/(μm)	Resolution (m)	Year	Acquisition Date
Landsat 5 TM	1—Blue 2—Green 3—Red 4—NIR	0.45–0.52 0.52–0.60 0.63–0.69 0.76–0.90	30	1991 1992 1996 1997 2004 2005 2006 2007 2008 2009 2010	12 September 1991 7 April 1992 7 July 1996 12 September 1997 14 August 2004 17 August 2005 4 August 2006 6 July 2007 6 June 2008 28 August 2009 3 May 2010
Landsat 7 ETM+	1—Blue 2—Green 3—Red 4—NIR	0.45–0.52 0.52–0.60 0.63–0.69 0.77–0.90	30	2000 2001 2002 2003	26 July 2000 26 May 2001 18 September 2002 19 July 2003
Landsat 8 OLI	2—Blue 3—Green 4—Red 5—NIR	0.45–0.51 0.53–0.59 0.64–0.67 0.85–0.88	30	2013 2014 2015 2016 2017 2018 2019 2020 2021	24 September 2013 23 June 2014 26 June 2015 16 September 2016 8 February 2017 4 July 2018 9 September 2019 26 August 2020 28 July 2021

3.2. Detection and Extraction of Shorelines

The present study follows a three-step procedure for identifying, delineating, and extracting the coastline of Oluvil from satellite images, using a geographic information system (GIS). The first step involved using the Normalized Difference Water Index (NDWI) method [78] as the spectral enhancement technique for Land–Water Classification, which is a commonly used algorithm providing good results. NDWI was calculated using Equation (1), which required adjustment for every Landsat image used due to the different wave spectra in each image (refer to Equation (1)).

$$\text{NDWI} = \frac{\text{Green} - \text{NIR}}{\text{Green} + \text{NIR}} \tag{1}$$

Here, NIR is the Near-Infrared wave band, and Green is the green band wave. The NDWI values were assumed to be interpreted as follows: values greater than zero indicated surfaces of water, while values lower than or equal to zero indicated non-water surfaces [78]. Next, the NDWI images were reclassified into binary format, where the value "1" represents water and "0" represents non-water surfaces. To extract the continuous edges of the coastline, the binary reclassified NDWI image was converted from raster to polygon/polyline, removing the edges of inland water bodies and retaining only the coastline (Refer to Figure 2). Finally, the extracted coastlines were smoothed to obtain accurate and reliable shoreline extraction results (Refer to Figure 3).
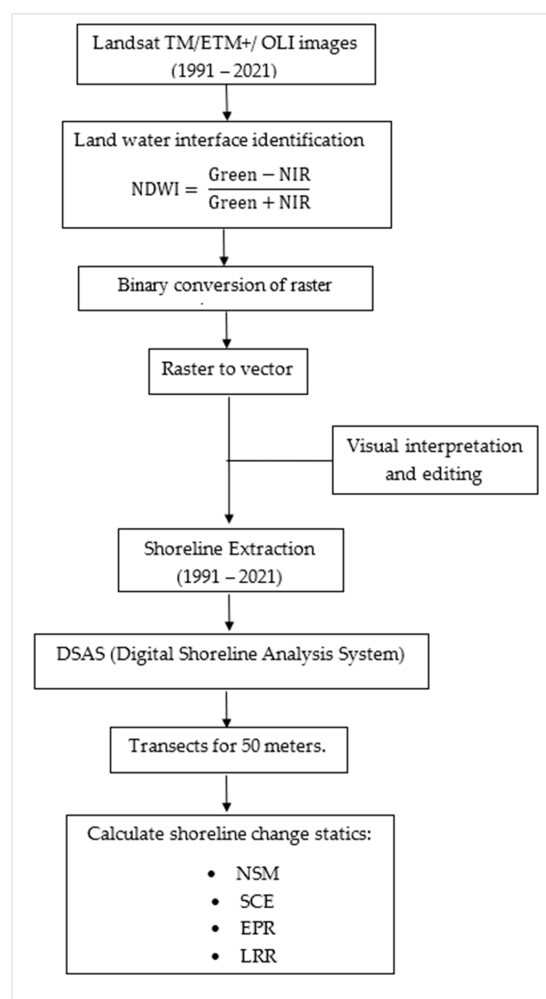
Figure 2. Schematic diagram of methodological procedures.
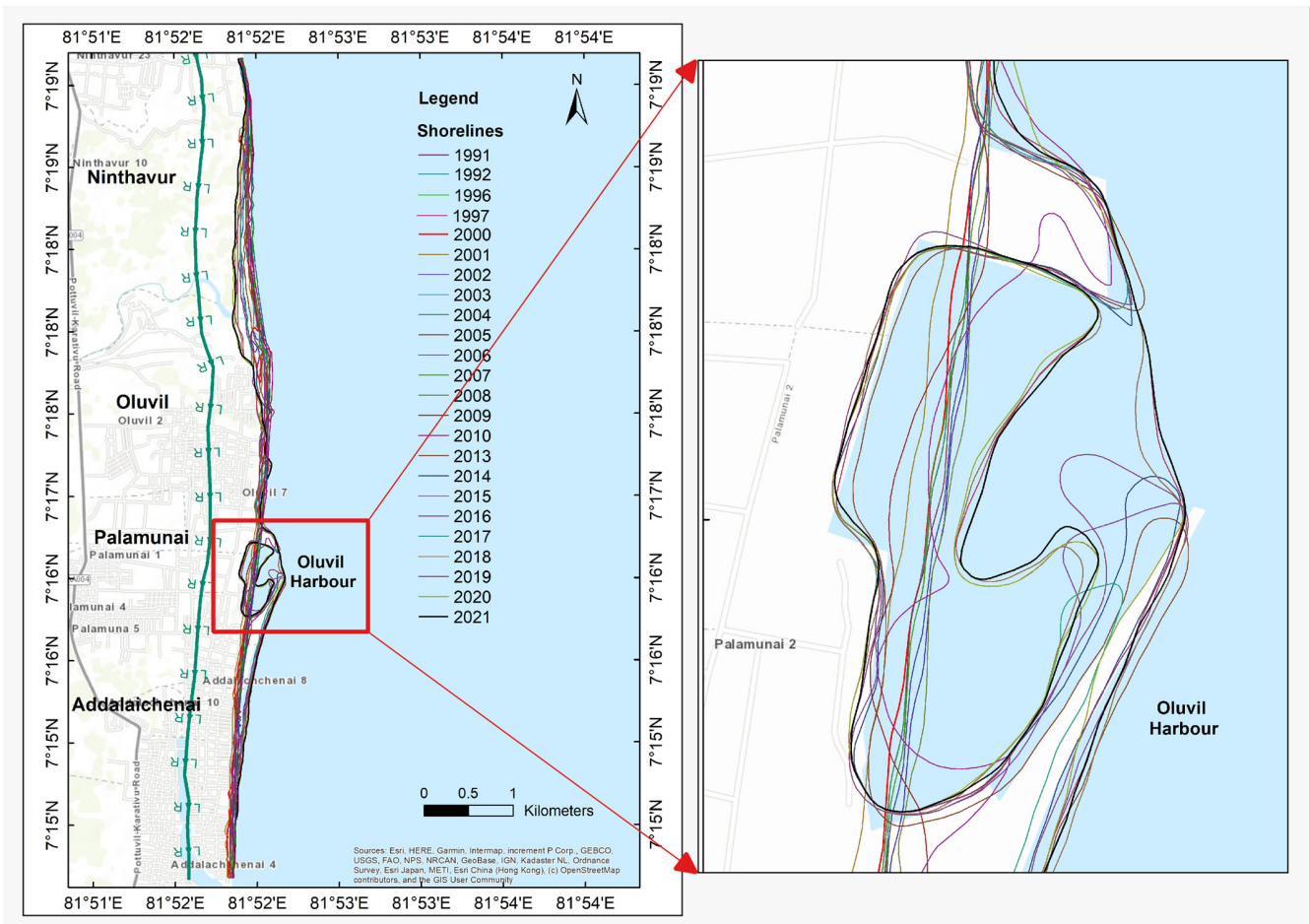
Figure 3. Extracted shorelines from Landsat satellite imageries (1991–2021).

3.3. The Digital Shoreline Analysis System (DSAS) Application

The Digital Shoreline Analysis System (DSAS) is an extension of ArcGIS software, developed by the U.S. Geological Survey, which enables the calculation of shoreline change statistics by measuring the differences between the extracted shorelines and baseline. This method has been used in numerous studies to determine temporal and spatial shoreline movements [50,79,80]. In the current study, Shoreline Change Envelope (SCE), the Net Shoreline Movement (NSM), End Point Rate (EPR), and Linear Regression Rate (LRR) were calculated using DSAS 5.0 and ArcGIS 10.7.1 to determine shoreline change statistics.

The NSM is calculated by subtracting the distance of the youngest shoreline from the oldest shoreline for each transect, with units in meters. Therefore, the NSM of a transect in this study can be calculated as in Equation (2). Hence, the NSM of a transect for the present study was calculated as given in Equation (3).

$$\text{NSM} = \text{Distance}(\text{Oldst shoreline} - \text{Youngest shoreline}) \tag{2}$$

$$\text{NSM} = \text{Distance}(\text{shoreline}_{2000} - \text{shoreline}_{2021}) \tag{3}$$

The SCE is the greatest distance between all the shorelines for a given transect; hence, it is always measured as a positive value relative to the baseline. This is calculated as given in Equation (4).

$$\text{SCE} = \text{Distance}(\text{Shoreline}_{\text{Farthest}} - \text{Shoreline}_{\text{Nearest}}) \tag{4}$$

The EPR was determined by dividing the NSM by the time interval between the oldest and youngest shorelines (T) and expressed the rate of change in meters per year (refer to Equation (5)).

$$\text{EPR} = \frac{\text{NSM}}{\text{T}} \tag{5}$$

LRR (m/year) was calculated by using a least square regression line from all shoreline positions along each transect. This method is useful for observing the trend of shoreline evolution and determining the linear regression rate, which corresponds to the long-term rates of coastal changes. Unlike the EPR method, the LRR method has the potential to use more than two shorelines, which helps to overcome the deficiency in EPR. The statistical results of the LRR were categorized into five groups based on the magnitude of shoreline changes: high accretion (>4 m/year), low accretion (1 to 4 m/year), stable (−1 to 1 m/year), low erosion (−4 to −1 m/year), and high erosion (>−4 m/year) following the method outlined by Velsamy et al. [81].

4. Results and Discussion

4.1. Changes in Shoreline Configuration Pre- and Post-Construction of Oluvil Harbor

Shoreline changes were observed to be within a normal range between 1991 and 2008. However, anomalous changes were noted in the study area between 2008 and 2021 (Refer to Figures 4 and 5). Hence, the construction of the harbor is believed to be the primary cause of these irregular shoreline changes, resulting in southward beach advancement and northward retreat in the vicinity of the Oluvil harbor (Refer to Figure 4).
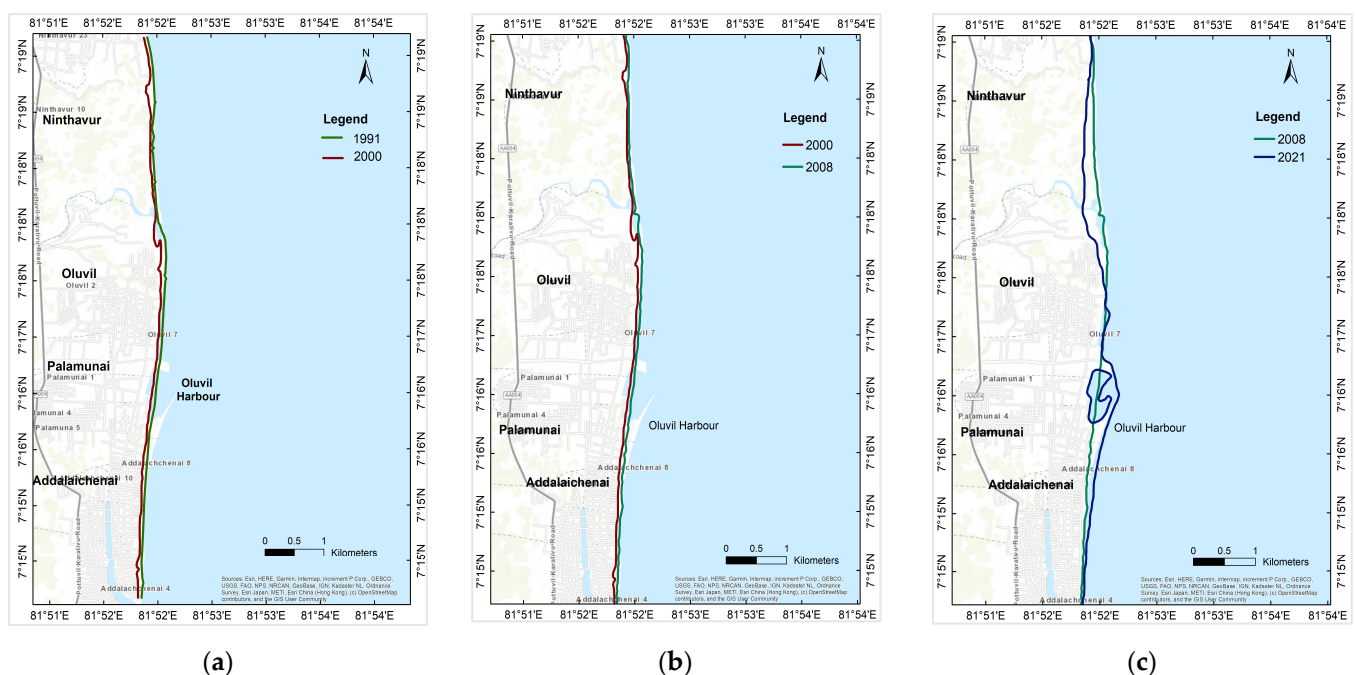
Figure 4. Spatial variation of Oluvil coastline trends: (**a**) For 1991–2000; (**b**) For 2000–2008; (**c**) For 2008–2021.

The effect of harbor jetties on coastal dynamics is readily apparent in both neighboring areas, where there was a rapid progradation of the shoreline and expansion of nearby beaches due to the gradual accumulation of sand against the jetties. The harbor interrupts both north and south longshore sediment transport, leading to the capture of sediment in its northern and southern sides and the deposition of sand in nearby beaches. However, accumulation rates decrease rapidly with increasing distance from the harbor.

Figure 5. Google Earth Pro Images used to study the periodic change of Oluvil Coastline from 2000–2021 (accessed on 30 December 2022).

During the early stages of harbor construction, the impact of the short piers on the shoreline configuration was minor (2008 shoreline). As the harbor expanded and the jetties were prolonged seaward, the coastline continued to shift, with transects building up on the south side of the harbor and shoreline retreat occurring on the northern side. Similar shoreline behaviors were noted in some other studies as well. For example, studies conducted on the Ravenna coastline variation (Italy) by Sytnik et al. [82] due to the construction of Marina di Ravenna harbor and at the Mediterranean coastline of the Gaza Strip [21] due to the Gaza harbor showed exactly the similar behavior.

4.2. DSAS Statics for Oluvil Coast

The current study quantified the rates of coastline change in each area of Oluvil from 1991 to 2021 developing 184 transects along the coastline to investigate the statistical

outputs of SCE, EPR, LRR, and NSM. The results of this study are presented in Figure 6a–d, where positive (+) and negative (−) values of NSM, EPR, and LRR indicate accretion and erosion, respectively, in a particular region.
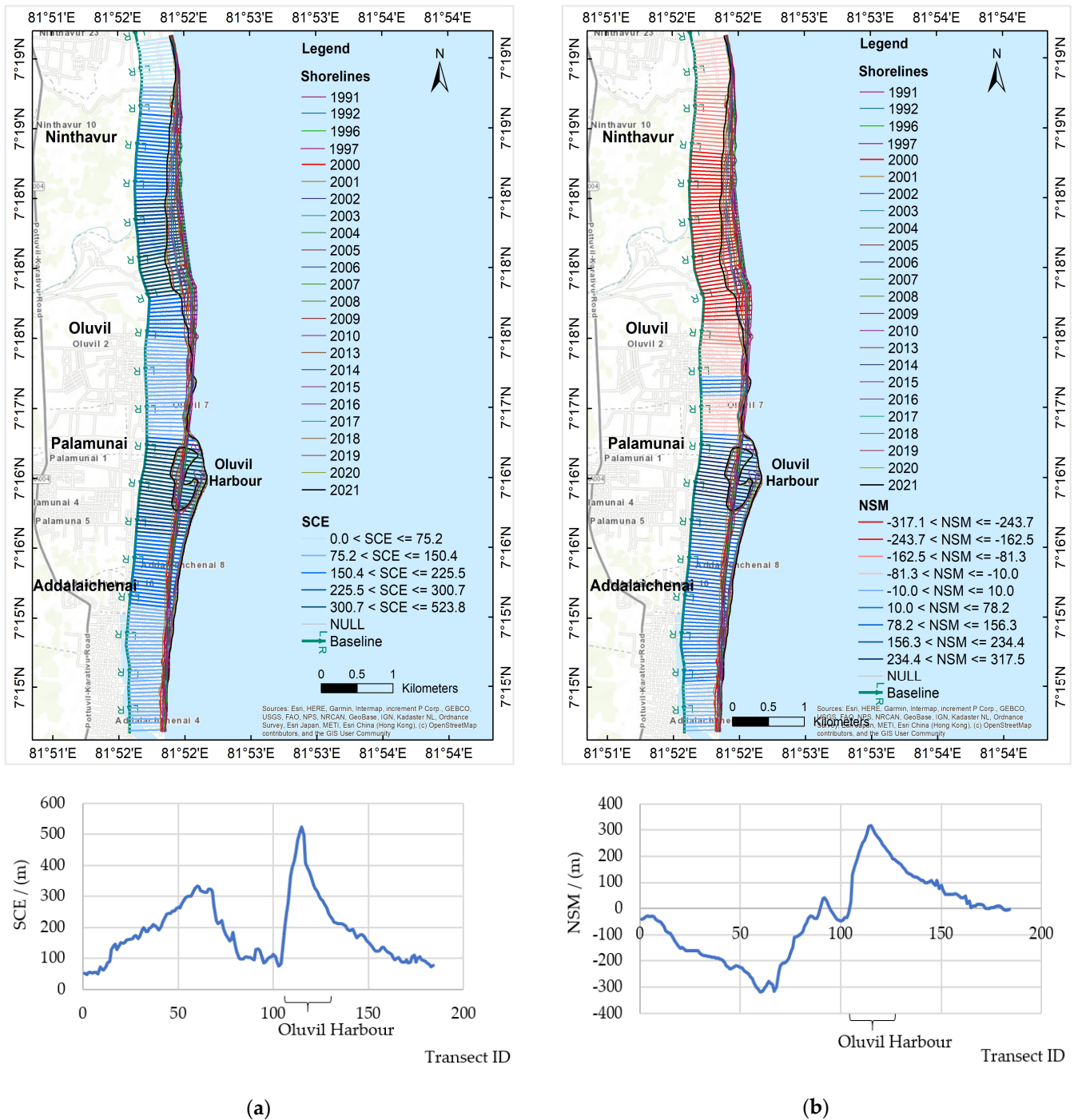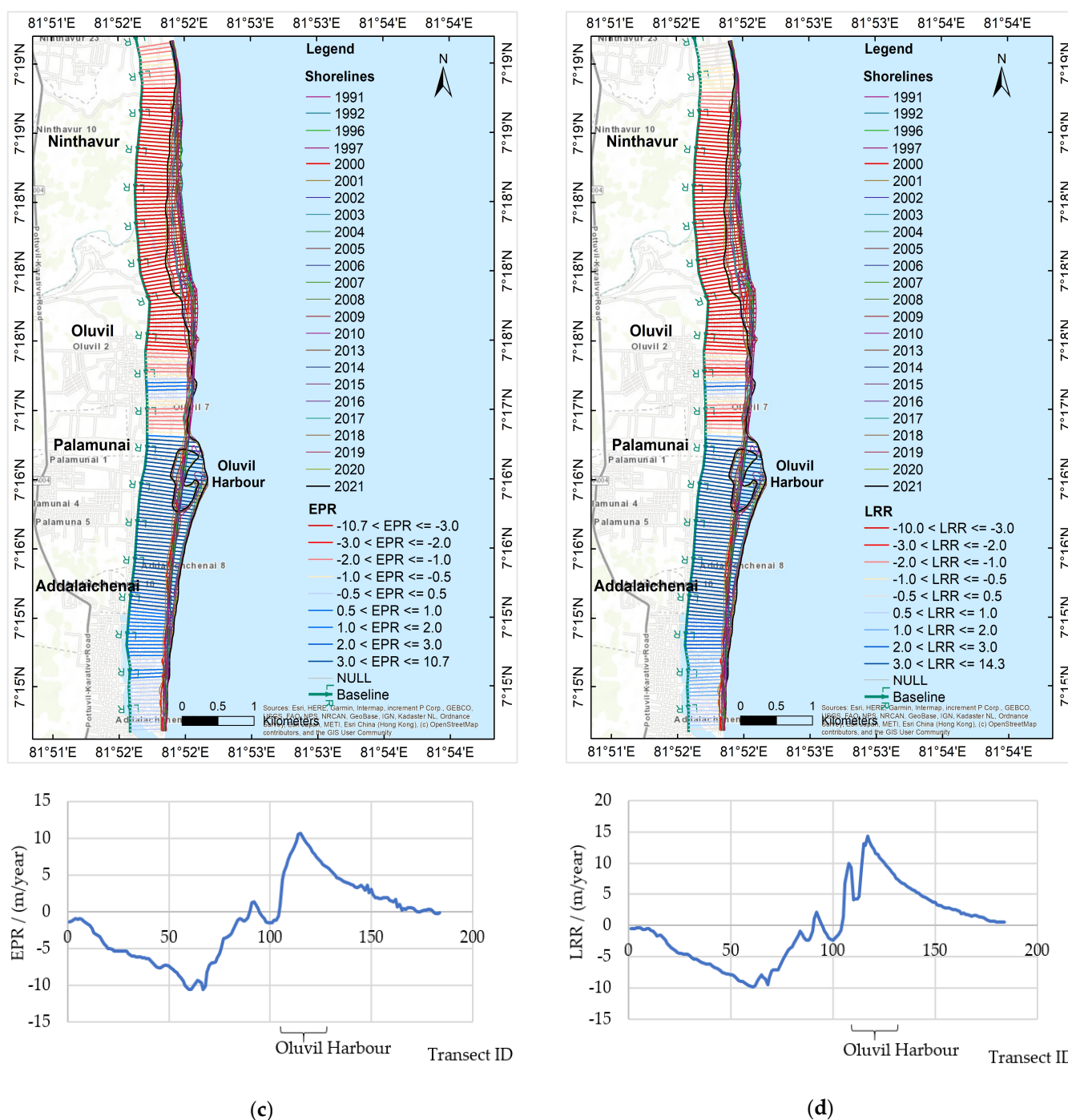

(a)

(b)

Figure 6. *Cont.*

(**c**)

(**d**)

Figure 6. DSAS Statics of the Oluvil coast area: (**a**) For SCE; (**b**) For NSM; (**c**) For EPR; (**d**) For LRR.

Two methods, SCE and NSM, were utilized to measure the distance of shoreline change and additional EPR and LRRs to calculate the rate of change (m/year). The LRR method uses all available shoreline positions from the considered past 30 years, while the EPR method only uses the oldest (1991) and youngest (2021) positions. Since LRR uses all the time series data, the impact from spurious values can be reduced on the overall accuracy of the change rate. Because of this, the LRR method is generally regarded as more reliable than the EPR method [83]. Based on the SCE results, during the study period of 1991–2021, the greatest shoreline change observed was 523.8 m, although it is important to note that this value could represent either accretion or erosion. However, it is worth noting that even though SCE values always result in positive values, the shoreline change

resulting from them does not necessarily indicate accretion. Transect number 115, situated within the Oluvil harbor region, recorded the farthest distance of shoreline change in the study area (refer to Figure 6a). On average, the distance between the farthest and closest shoreline shift to the baseline was 187.3 m.

The study area's resulting NSM values revealed severe erosion in the Oluvil area with values ranging from −317.02 to +317.47 m (refer to Figure 6b). In the Ninthavur region, NSM values range from −243.7 to −81.3 m, also indicating considerable erosion. On the other hand, the Palamunai area, which is closest to the harbor in the southward direction, recorded the highest variation in NSM of 10–317.5 m, indicating significant accretion. A tail-like sedimentation shape has formed in the southward direction to the harbor (refer to Figure 5), with NSM values ranging from 10–156.3 m, extending southward. Within the area of transition, where erosion and accretion are in flux, NSM values range from −81.3 to −10 m and −10 to 78.2 m, with negative and positive values indicating both erosion and accretion scenarios.

The EPR analysis indicates that the maximum accumulation rates occur between 3 m/year to 10.7 m/year southward of the harbor, while the highest levels of beach erosion were recorded between −10.7 m/year to −3.0 m/year northward direction of the harbor (Refer to Figure 6c). From 1991 to 2008, the shoreline remained relatively stable (refer to Figure 4). However, since the start of harbor construction in 2008, major changes have been observed in the post-construction period of 2008–2021, with anomalous erosion and accretion occurring in the regions north and south of the harbor.

The LRR rates calculated in this study reveal the rate of shoreline change per year (refer to Figure 6d). The analysis shows that anomalous erosion with rates ranging from −3 m/year to −10 m/year occurred northward of the harbor, resulting in beach retrogradation. On the other hand, southward of the harbor, beach progradation was observed at rates of 3 m/year to 14.3 m/year. As stated by Velsamy et al. [81], the Oluvil coast has experienced significant erosion and accretion (Refer to Figure 6d), with values exceeding 4 m per year.

The DSAS kinematics depicted that shoreline changes on both sides of the harbor have a trend of increasing landward (seaward) movement in the northward (southward) area over time. These findings from monitoring and measuring the distance and rate of shoreline changes on Sri Lanka's eastern coast are important for the effective management, protection, and conservation of coastal resources. Reliable assessment of the present-day wave climate and erosion hotspots in the study area is challenging due to the unavailability of local wave measurements. Therefore, the authors recommend conducting future studies to validate the results obtained in this study.

4.3. Dynamic Shoreline Processes: Erosion and Accretion

Figure 7 illustrates the changes in eroded and accreted areas along the Oluvil coast during the period of 2008–2021. In the study period, the northern regions of the Oluvil harbor experienced erosion, while the southern regions experienced accretion. Erosion was especially strong in the estuarine areas, where the total length of eroded sections was 4150 m, and the area was 40 ha. The total length of accreted sections was 5545 m with an area of 84.44 ha. The strongest eroded section was observed in the north of the Oluvil harbor along the Ninthavur-Oluvil coastline (refer to Figures 7 and 8). In contrast, the most accretion section was in the south of the Oluvil harbor along the Palamunai–Addalachenai coastline (refer to Figures 7 and 8). These changes suggest that the breakwaters at the harbor entrance are impeding longshore sediment delivery, resulting in accumulation within the harbor opening and along the southward route of the harbor, which includes Palamunai and Addalaichenai beaches.
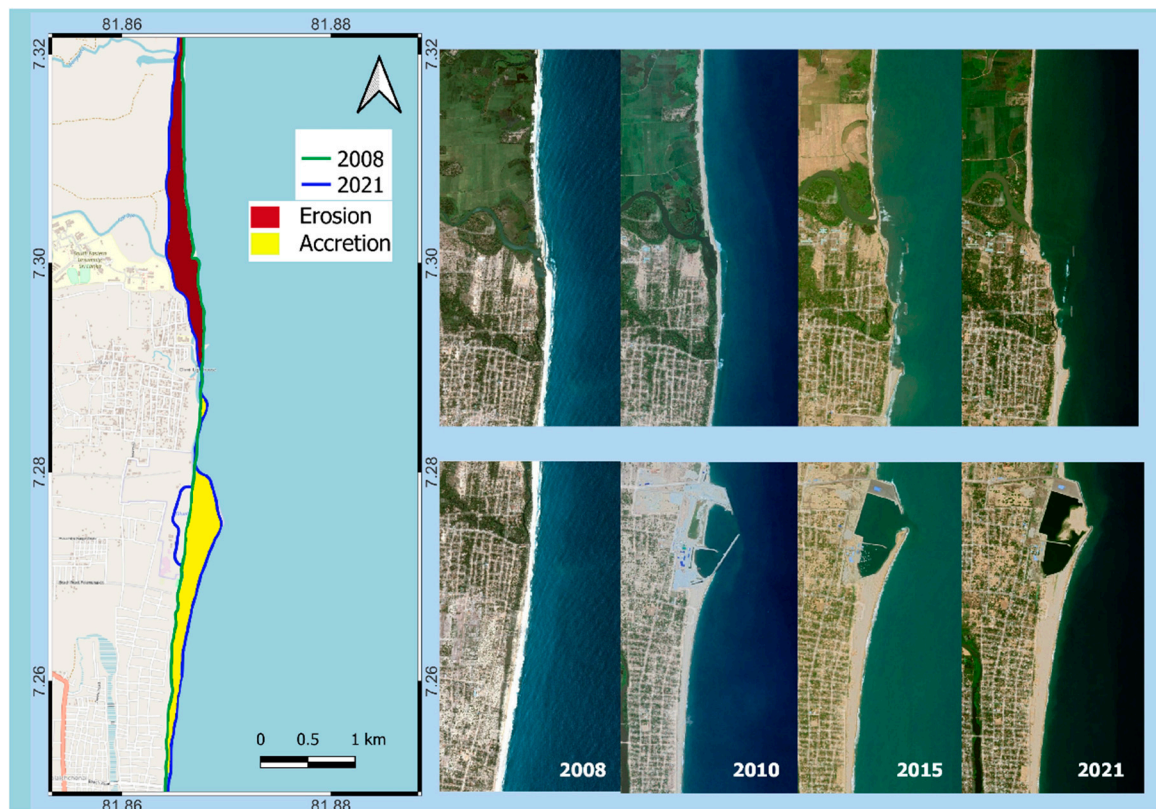
Figure 7. Eroded and accreted areas in the Oluvil coast during 2008–2021 (accessed on 30 December 2022).

Figure 8. Eroded and accreted areas in the Oluvil coastline (accessed on 7 January 2023).

4.4. Potential Impact of Shoreline Changes on Eco-System and Land Use Patterns

The study area is encompassed by an array of natural habitats such as beaches, lagoons, and mangroves, all of which support a rich biodiversity. Hence, this area is sensitive to both flora and fauna. For example, this area is home to the critically endangered *Sesamum prostratum*, which is listed in the 2012 national red data book. *Scaevola plumieri* (Heen Takkada), which is a rare plant species within the country, can also be found in this area. Additionally, endemic plant species such as *Vernonia zeylanica* (Pupulu), *Cassine glauca* (Neralu), and *Derris parviflora* (Kala Wel) also have been reported in the area. This region not only houses plant species, but also migratory birds such as the blue-tailed bee-eater (*Merops philippinus*) (the blue-tailed bee-eater has been classified as Critically Endangered due to the limited breeding population within Sri Lanka). A new breeding location for the blue-tailed bee-eater in the vicinity of Oluvil Harbor has been discovered [84]. He further stated that due to Oluvil harbor construction, artificial sand dunes have become the largest nesting area observed on the island for this migratory bird species. However, the construction of the Oluvil Harbor has caused numerous problems for the area and the environment. While the development was intended to provide benefits to society and the government, it has resulted in numerous complications. Before 2008, the locals were engaged in agricultural and fishing activities. The farmers and fishermen reaped benefits both economically and physically. The northern part of the harbor consisted of 30 acres of agricultural land, where over 4000 coconut trees were planted, and paddy and vegetables were productively cultivated. They also have used traditional fishing methods and earned substantial income from deep sea fishing during each season. They also conducted freshwater fishing in Kali-odai River for a long period [85].

However, after the harbor project, the locals faced a host of new challenges. Erosion occurred more on the north side of the harbor, while accumulation was observed on the south side affecting the eco-system of these coastal areas. The primary issue is coastal erosion, which has continued since the harbor development began. Currently, more than 100 m of land have retreated near the sea, and more than 3000 coconut trees have been destroyed due to erosion. Additionally, 30 acres of land remain abandoned without any cultivation [86]. Moreover, the construction of the port has resulted in the blockage of the irrigation channel for the paddy lands. This has led to the ingress of seawater into the paddy lands via the river, causing erosion and resulting in the loss of paddy lands to the sea [86].

Fish resources were also affected by the harbor's development, causing a significant reduction in the quantity of fish. The erosion caused a change in the mouth of Kali-odai River, leading to the loss of livelihood for around 500 to 1000 fishermen [86]. The authorities attempted to address erosion by constructing wave barriers using granite on the shoreline, but this solution proved to be inadequate, causing additional erosion and resulting in the destruction of 20 fishing boats [86,87]. This has also resulted in the loss of the natural coastline that fishermen relied on for their livelihoods. Consequently, both traditional fishermen and those using conventional fishing crafts lost access to the coast for their activities, making it impossible to continue their occupation.

Additionally, the coastal vegetation in these areas provided a seasonal habitat for turtles to lay their eggs and propagate new generations. However, erosion has destroyed this vegetation, which has disrupted the turtles' reproductive patterns and caused them to stop coming to these areas [86].

This has rendered the harbor ineffective in achieving its construction goals. Sediment from the northern region is being carried away and deposited along the southern part of the Oluvil harbor. The accretion has also caused siltation at the mouth of the Oluvil harbor, resulting in vessel operation being at a standstill. Therefore, it is necessary to stabilize and achieve sustainable improvement of the Oluvil coastal region.

4.5. Current State of Oluvil Harbor and Potential Strategies for Future Mitigations

The Oluvil Harbor was constructed to achieve specific objectives including the provision of proper port services for commercial ships, the enhancement of coastal access, and the improvement of the coastal route. Another important goal was to attract investors through increased fishing, which would lead to more employment opportunities and address issues faced by deep sea fishing vessels. However, despite the completion of the project in 2013, the harbor and all associated buildings remained inactive for over eight years due to environmental challenges, notably sea erosion that worsened following the harbor's construction. This situation led to the development of a breakwater arrangement to obstruct the seawater flow. However, this blocked the sand flow, leading to sea erosion in the northern area and sand accumulation at the port's entrance preventing fishing boats from entering the sea from the fishing harbor. Due to the severity of the sand accumulation, fishing boats cannot enter the sea from the fishing harbor, leading to the suspension of its operation since September 2018. Therefore, no ship has utilized the commercial port to date. However, temporary dredging is performed at the port entrance to facilitate the entrance requirements of local fishermen. It should be noted that this is a short-term measure intended solely for addressing this particular situation. The boats and ships purchased with the expectation of utilizing the fishing harbor are currently anchored in Valaichenai, causing a significant hardship for local fishermen.

To resume fishing activities in Oluvil harbor, it is necessary to remove the sand deposits at the entrance of the port. However, dredging is not a viable long-term solution due to its cost implications. Unfortunately, the lack of local wave measurements and morphological data in the study area makes it difficult to identify and quantify longshore sediment transport and erosion hotspots. Most available studies have focused on the southwestern coasts of Sri Lanka, with a few conducted on the eastern coast. For example, Nijamir and Kaleel [86] propose several measures to manage shoreline erosion in the Oluvil coastal area. These include expanding the breakwater's coverage area through the use of multiple small, detached segments, utilizing a wave-attenuation system such as a floating breakwater, safeguarding mangroves, installing rift fences to regulate wind erosion, implementing concrete interlocking pieces, and replanting to manage shoreline changes. However, to arrive at a permanent solution, collecting data on sea waves over the past three years and analyzing them with advanced techniques such as long-term observation-based numerical models is crucial, which is also concluded by Nijamir and Kaleel [86]. This will enable a proper understanding of wave transformation and sediment transport modeling in the study area and the reliable assessment of present-day longshore sediment transport, wave climate, and erosion hotspots. Further, Nijamir and Kaleel [86] have stated that it is also important to implement nationally or internationally recognized integrated coastal zone management (ICZM) processes within the study area. These will aid in deciding on a proper solution for the current problem. Consequently, a sustainable solution can be decided based on a proper environmental impact assessment.

4.6. Accuracy of LandSat Images in the Shoreline Detection

The accuracy of the LandSat images is always questionable in the context of shoreline detention. Cloud cover and resolution can be major concerns that are affecting the accuracy of the LandSat images. However, it is difficult to assess the accuracy when it comes to shoreline changes in some counties due to poor ground measurements. Most developing countries do not have a direct monitoring system to measure and record the shoreline to showcase the spatiotemporal variation. The data scatter on this is very poor in Sri Lanka. Therefore, the accuracy of the LandSats in the context of Sri Lankan shores is not compared yet. Nevertheless, literature gives many similar studies showcasing the higher accuracy of the LandSat images in the context of shoreline assessment. Apostolopoulos and Nikolakopoulos [41] assessed and quantified the accuracy of remote sensing data for shoreline monitoring. They identified the lower spatial resolution of Landsat images as the major drawback. Pardo–Pascual et al. [43] assessed the accuracy of Landsat 7, Landsat

8, and Sentinel−2 images in relation to shoreline prediction of the Valencian coast. Their results suggested that mean horizontal errors of 3.06–5.50 m can be observed in these satellite images. In addition, the mean annual shorelines in 9 km of sandy beach at El Saler, Valencia, Spain were assessed by Almonacid–Caballer et al. [87]. They observed 4–5 m of seaward error in Landsats in comparison to the more precise methods. Nevertheless, Karaman [88] showcases higher accuracies in satellite images for shoreline protection on Lake Salda, Turkey. Similar results were found by Dewidar and Bayoumi [89] in their research work, which had 31 Landsat images. Therefore, it can be clearly seen herein that the Landsat images are heavily used in the related studies even at a cost of some accuracy. The usage of Landsat is significant in the data scarcity regions. However, accuracy can be enhanced by using higher-resolution satellite images. Nevertheless, the authorities should be willing to incur the cost of higher-resolution satellite images for such cases.

5. Conclusions and Future Works

This study employed Landsat images and the GIS tool DSAS to detect periodic shoreline changes in the Oluvil Coast in Ampara district, Sri Lanka. The findings indicated that the shorelines have been undergoing temporal shifting, with the periodical accretion of surrounding beaches occurring in the southward area of the harbor, and a landward movement of the sea from the northward area of the Oluvil harbor. Upon analyzing the areas affected by shoreline retreat, it can be inferred that the shape of the Oluvil coast has undergone significant variations due to human-induced harbor constructions.

The observed changes between 2008 and 2021 have significantly affected the socioeconomic environment of the Oluvil region. The livelihoods of subsistence fishers, who relied on coastline fisheries, have been detrimentally impacted due to cottage destruction caused by shoreline changes. Coastal erosion also has destroyed coconut farmland, affecting the socio-economic stability of the landowners' income. Therefore, proper shoreline protective measures should be implemented to mitigate and control the present shoreline changes, thereby curbing future trends and their impact on society. This study also highlights the critical importance of conducting thorough hydro and morphodynamic analyses prior to the implementation of large engineering projects near coastlines. It further documented that neglecting these analyses can result in significant losses and negative consequences for both local communities and the environment, indicating the difficulties in remedying damages once they have already occurred. Overall, this research highlights the critical role of scientific inquiry and responsible decision-making in promoting sustainable development and protecting communities and the environment.

The present study primarily focuses on the anthropogenic effect. However, It is important to acknowledge that natural factors can also contribute to shoreline erosion. Therefore, it is recommended that future shoreline analyses incorporate natural factors to produce more accurate and comprehensive results for comparison. Conducting future studies to validate the results obtained in this study is also another recommendation arrived at through the present study.

Author Contributions: Conceptualization, U.R.; methodology, S.Z. and V.B.; software, S.Z. and V.B.; validation, J.T.S., M.B.G., K.K. and U.P.; formal analysis, S.Z. and V.B.; investigation, S.Z. and V.B.; resources, S.Z. and V.B.; data curation, S.Z., V.B., J.T.S. and M.B.G.; writing—original draft preparation, S.Z. and V.B.; writing—review and editing, K.K., N.M., U.P. and U.R.; visualization, S.Z.; supervision, J.T.S., M.B.G. and U.R.; project administration, U.R. All authors have read and agreed to the published version of the manuscript.

Institutional Review Board Statement: Not applicable.

Informed Consent Statement: Not applicable.

Data Availability Statement: Data is available on request from the corresponding author.

References

1. Crossland, C.J.; Kremer, H.H.; Lindeboom, H.; Crossland, J.I.M.; Le Tissier, M.D. (Eds.) *Coastal Fluxes in the Anthropocene: The Land-Ocean Interactions in the Coastal Zone Project of the International Geosphere-Biosphere Programme*; Springer Science & Business Media: Berlin/Heidelberg, Germany, 2005.
2. McGranahan, G.; Balk, D.; Anderson, B. The rising tide: Assessing the risks of climate change and human settlements in low elevation coastal zones. *Environ. Urban.* **2007**, *19*, 17–37. [CrossRef]
3. Cenci, L.; Disperati, L.; Persichillo, M.G.; Oliveira, E.R.; Alves, F.L.; Phillips, M. Integrating remote sensing and GIS techniques for monitoring and modeling shoreline evolution to support coastal risk management. *GISci. Remote Sens.* **2018**, *55*, 355–375. [CrossRef]
4. Kummu, M.; De Moel, H.; Salvucci, G.; Viviroli, D.; Ward, P.J.; Varis, O. Over the hills and further away from coast: Global geospatial patterns of human and environment over the 20th–21st centuries. *Environ. Res. Lett.* **2016**, *11*, 034010. [CrossRef]
5. Franco-Ochoa, C.; Zambrano-Medina, Y.; Plata-Rocha, W.; Monjardín-Armenta, S.; Rodríguez-Cueto, Y.; Escudero, M.; Mendoza, E. Long-term analysis of wave climate and shoreline change along the Gulf of California. *Appl. Sci.* **2020**, *10*, 8719. [CrossRef]
6. Del Río, L.; Gracia, F.J.; Benavente, J. Shoreline change patterns in sandy coasts. A case study in SW Spain. *Geomorphology* **2013**, *196*, 252–266. [CrossRef]
7. Palamakumbure, L.; Ratnayake, A.S.; Premasiri, H.M.R.; Ratnayake, N.P.; Katupotha, J.; Dushyantha, N.; Weththasinghe, S.; Weerakoon, W.A.P. Sea-level inundation and risk assessment along the south and southwest coasts of Sri Lanka. *Geoenviron. Disasters* **2020**, *7*, 17. [CrossRef]
8. Reise, K. Coast of change: Habitat loss and transformations in the Wadden Sea. *Helgol. Mar. Res.* **2005**, *59*, 9–21. [CrossRef]
9. Jacob, C.; Bernatchez, P.; Dupras, J.; Cusson, M. Not just an engineering problem: The role of knowledge and understanding of ecosystem services for adaptive management of coastal erosion. *Ecosyst. Serv.* **2021**, *51*, 101349. [CrossRef]
10. Lanka, S.; Lewangamage, C.; Lewangamage, S.; Srisangeerthanan, S. Tropical cyclone damages in Sri Lanka. *Wind Eng. JAWE* **2015**, *40*, 294–302.
11. Parape, C.D.; Premachandra, C.; Tamura, M.; Bari, A.; Disanayake, R.; Welikanna, D.; Jin, S.; Sugiura, M. Building damage and business continuity management in the event of natural hazards: Case study of the 2004 tsunami in Sri Lanka. *Sustainability* **2013**, *5*, 456–477. [CrossRef]
12. Illangasekare, T.; Tyler, S.W.; Clement, T.P.; Villholth, K.G.; Perera, A.P.G.R.L.; Obeysekera, J.; Gunatilaka, A.; Panabokke, C.R.; Hyndman, D.W.; Cunningham, K.J.; et al. Impacts of the 2004 tsunami on groundwater resources in Sri Lanka. *Water Resour. Res.* **2006**, *42*, 1–9. [CrossRef]
13. Poisson, B.; Garcin, M.; Pedreros, R. The 2004 December 26 Indian Ocean tsunami impact on Sri Lanka: Cascade modelling from ocean to city scales. *Geophys. J. Int.* **2009**, *177*, 1080–1090. [CrossRef]
14. Chandrasekara, S.S.K.; Uranchimeg, S.; Kwon, H.H.; Lee, S.O. Coastal Flood Disaster in Sri Lanka-May 2017: Exploring Distributional Changes in Rainfall and Their Impacts on Flood Risk. *J. Coast. Res.* **2018**, *85*, 1476–1480. [CrossRef]
15. Pollard, J.A.; Spencer, T.; Brooks, S.M. The interactive relationship between coastal erosion and flood risk. *Prog. Phys. Geogr.* **2019**, *43*, 574–585. [CrossRef]
16. Alpar, B. Vulnerability of Turkish coasts to accelerated sea-level rise. *Geomorphology* **2009**, *107*, 58–63. [CrossRef]
17. Chandrasekar, N. Coastal Vulnerability and Shoreline Changes for Southern Tip of India-Remote Sensing and GIS Approach. *J. Earth Sci. Clim. Chang.* **2013**, *4*, 2. [CrossRef]
18. Murali, R.M.; Dhiman, R.; Choudhary, R.; Seelam, J.K.; Ilangovan, D.; Vethamony, P. Decadal shoreline assessment using remote sensing along the central Odisha coast, India. *Environ. Earth Sci.* **2015**, *74*, 7201–7213. [CrossRef]
19. Dean, R.G.; Galvin, C.J., Jr. Beach erosion: Causes, processes, and remedial measures. *Crit. Rev. Environ. Sci. Technol.* **1976**, *6*, 259–296. [CrossRef]
20. Aladwani, N.S. Shoreline change rate dynamics analysis and prediction of future positions using satellite imagery for the southern coast of Kuwait: A case study. *Oceanologia* **2022**, *64*, 417–432. [CrossRef]
21. Abualtayef, M.; Ghabayen, S.; Foul, A.A.; Seif, A.; Kuroiwa, M.; Matsubara, Y.; Matar, O. The Impact of Gaza Fishing Harbour on the Mediterranean Coast of Gaza. *J. Coast. Zone Manag.* **2012**, *16*, 1–10. Available online: https://www.neliti.com/publications/92470/ (accessed on 30 November 2022).
22. CCCRMD. *Sri Lanka Coastal Zone and Coastal Resource Management Plan (CZMP)—2018*; CCCRMD: Silver Spring, MD, USA, 2018.
23. Stockdon, H.F.; Sallenger, A.H.; List, J.H.; Holman, R.A. Estimation of shoreline position and change using airborne topographic lidar data. *J. Coast. Res.* **2002**, *18*, 502–513.
24. Mapping, S.; Moore, L.J. Shoreline Mapping Techniques. *J. Coast. Res.* **2000**, *16*, 111–124.

25. Basterretxea, G.; Orfila, A.; Jordi, A.; Fornós, J.J.; Tintoré, J. Evaluation of a small volume renourishment strategy on a narrow Mediterranean beach. *Geomorphology* **2007**, *88*, 139–151. [CrossRef]

26. Jones, B.M.; Arp, C.D.; Jorgenson, M.T.; Hinkel, K.M.; Schmutz, J.A.; Flint, P.L. Increase in the rate and uniformity of coastline erosion in Arctic Alaska. *Geophys. Res. Lett.* **2009**, *36*, 1–5. [CrossRef]

27. Murray, J.; Adam, E.; Woodborne, S.; Miller, D.; Xulu, S.; Evans, M. Monitoring shoreline changes along the southwestern coast of South Africa from 1937 to 2020 using varied remote sensing data and approaches. *Remote Sens.* **2023**, *15*, 317. [CrossRef]

28. Wang, J.; Wang, L.; Feng, S.; Peng, B.; Huang, L.; Fatholahi, S.N.; Tang, L.; Li, J. An Overview of Shoreline Mapping by Using Airborne LiDAR. *Remote Sens.* **2023**, *15*, 253. [CrossRef]

29. White, S.A.; Wang, Y. Utilizing DEMs derived from LIDAR data to analyze morphologic change in the North Carolina coastline. *Remote Sens. Environ.* **2003**, *85*, 39–47. [CrossRef]

30. Yang, B.; Hwang, C.; Cordell, H.K. Use of LiDAR shoreline extraction for analyzing revetment rock beach protection: A case study of Jekyll Island State Park, USA. *Ocean Coast. Manag.* **2012**, *69*, 1–15. [CrossRef]

31. Smeeckaert, J.; Mallet, C.; David, N.; Chehata, N.; Ferraz, A. Large-scale classification of water areas using airborne topographic lidar data. *Remote Sens. Environ.* **2013**, *138*, 134–148. [CrossRef]

32. Gens, R. Remote sensing of coastlines: Detection, extraction and monitoring. *Int. J. Remote Sens.* **2010**, *31*, 1819–1836. [CrossRef]

33. Dellepiane, S.; De Laurentiis, R.; Giordano, F. Coastline extraction from SAR images and a method for the evaluation of the coastline precision. *Pattern Recognit. Lett.* **2004**, *25*, 1461–1470. [CrossRef]

34. Trebossen, H.; Deffontaines, B.; Classeau, N.; Kouame, J.; Rudant, J.P. Suivi des évolutions côtières et des risques littoraux en Guyane française par imagerie radar à synthèse d'ouverture. *C. R. Geosci.* **2005**, *337*, 1140–1153. [CrossRef]

35. Maiti, S.; Bhattacharya, A.K. Shoreline change analysis and its application to prediction: A remote sensing and statistics based approach. *Mar. Geol.* **2009**, *257*, 11–23. [CrossRef]

36. Liu, Y.; Huang, H.; Qiu, Z.; Fan, J. Detecting coastline change from satellite images based on beach slope estimation in a tidal flat. *Int. J. Appl. Earth Obs. Geoinf.* **2013**, *23*, 165–176. [CrossRef]

37. Kuleli, T.; Guneroglu, A.; Karsli, F.; Dihkan, M. Automatic detection of shoreline change on coastal Ramsar wetlands of Turkey. *Ocean Eng.* **2011**, *38*, 1141–1149. [CrossRef]

38. Pardo-Pascual, J.E.; Almonacid-Caballer, J.; Ruiz, L.A.; Palomar-Vázquez, J. Automatic extraction of shorelines from Landsat TM and ETM+ multi-temporal images with subpixel precision. *Remote Sens. Environ.* **2012**, *123*, 1–11. [CrossRef]

39. Li, W.; Gong, P. Continuous monitoring of coastline dynamics in western Florida with a 30-year time series of Landsat imagery. *Remote Sens. Environ.* **2016**, *179*, 196–209. [CrossRef]

40. Gerardo, R.; de Lima, I. Comparing the capability of sentinel-2 and Landsat 9 imagery for mapping water and sandbars in the river bed of the Lower Tagus River (Portugal). *Remote Sens.* **2023**, *15*, 1927. [CrossRef]

41. Apostolopoulos, D.N.; Nikolakopoulos, K.G. Assessment and quantification of the accuracy of low-and high-resolution remote sensing data for shoreline monitoring. *ISPRS Int. J. Geo-Inf.* **2020**, *9*, 391. [CrossRef]

42. Hagenaars, G.; de Vries, S.; Luijendijk, A.P.; de Boer, W.P.; Reniers, A.J.H.M. On the accuracy of automated shoreline detection derived from satellite imagery: A case study of the sand motor mega-scale nourishment. *Coast. Eng.* **2018**, *133*, 113–125. [CrossRef]

43. Pardo-Pascual, J.E.; Sánchez-García, E.; Almonacid-Caballer, J.; Palomar-Vázquez, J.M.; de los Santos, E.P.; Fernández-Sarría, A.; Balaguer-Beser, Á. Assessing the accuracy of automatically extracted shorelines on microtidal beaches from landsat 7, landsat 8 and sentinel-2 imagery. *Remote Sens.* **2018**, *10*, 326. [CrossRef]

44. Viaña-Borja, S.P.; Ortega-Sánchez, M. Automatic methodology to detect the coastline from Landsat images with a new water index assessed on three different Spanish Mediterranean deltas. *Remote Sens.* **2019**, *11*, 2186. [CrossRef]

45. Kuleli, T. Quantitative analysis of shoreline changes at the mediterranean coast in Turkey. *Environ. Monit. Assess.* **2010**, *167*, 387–397. [CrossRef] [PubMed]

46. Yadav, A.; Dodamani, B.M.; Dwarakish, G.S. Shoreline analysis using Landsat-8 satellite image. *ISH J. Hydraul. Eng.* **2021**, *27*, 347–355. [CrossRef]

47. Pham, B.T.; Prakash, I. Application of simple remote sensing techniques for the detection and extraction of coastline-a case study of diu island, India. *Indian J. Ecol.* **2018**, *45*, 778–784.

48. Immanuvel David, T.; Mukesh, M.V.; Kumaravel, S.; Sabeen, H.M. Long-and short-term variations in shore morphology of Van Island in gulf of Mannar using remote sensing images and DSAS analysis. *Arab. J. Geosci.* **2016**, *9*, 756. [CrossRef]

49. Otmani, H.; Belkessa, R.; Bengoufa, S.; Boukhediche, W.; Djerrai, N.; Abbad, K. Assessment of shoreline dynamics on the Eastern Coast of Algiers (Algeria): A spatiotemporal analysis using in situ measurements and geospatial tools. *Arab. J. Geosci.* **2020**, *13*, 124. [CrossRef]

50. Thieler, E.R.; Himmelstoss, E.A.; Zichichi, J.L.; Ergul, A. The Digital Shoreline Analysis System (DSAS) Version 4.0—An ArcGIS extension for calculating shoreline change. In *Open-File Report*; US Geological Survey: Reston, VA, USA, 2009. [CrossRef]

51. Boak, E.H.; Turner, I.L. Shoreline definition and detection: A review. *J. Coast. Res.* **2005**, *21*, 688–703. [CrossRef]

52. Markose, V.J.; Rajan, B.; Kankara, R.S.; Chenthamil Selvan, S.; Dhanalakshmi, S. Quantitative analysis of temporal variations on shoreline change pattern along Ganjam district, Odisha, east coast of India. *Environ. Earth Sci.* **2016**, *75*, 929. [CrossRef]

53. Hou, X.Y.; Wu, T.; Hou, W.; Chen, Q.; Wang, Y.D.; Yu, L.J. Characteristics of coastline changes in mainland China since the early 1940s. *Sci. China Earth Sci.* **2016**, *59*, 1791–1802. [CrossRef]

54. Mahapatra, M.; Ratheesh, R.; Rajawat, A.S. Shoreline Change Analysis along the Coast of South Gujarat, India, Using Digital Shoreline Analysis System. *J. Indian Soc. Remote Sens.* **2014**, *42*, 869–876. [CrossRef]

55. Liu, H.; Jezek, K.C. Automated extraction of coastline from satellite imagery by integrating Canny edge detection and locally adaptive thresholding methods. *Int. J. Remote Sens.* **2004**, *25*, 937–958. [CrossRef]

56. El-Asmar, H.M.; White, K. Changes in coastal sediment transport processes due to construction of New Damietta Harbour, Nile Delta, Egypt. *Coast. Eng.* **2002**, *46*, 127–138. [CrossRef]

57. Sun, F.; Sun, W.; Chen, J.; Gong, P. Comparison and improvement of methods for identifying waterbodies in remotely sensed imagery. *Int. J. Remote Sens.* **2012**, *33*, 6854–6875. [CrossRef]

58. Modava, M.; Akbarizadeh, G.; Soroosh, M. Integration of Spectral Histogram and Level Set for Coastline Detection in SAR Images. *IEEE Trans. Aerosp. Electron. Syst.* **2019**, *55*, 810–819. [CrossRef]

59. Yang, Y.; Liu, Y.; Zhou, M.; Zhang, S.; Zhan, W.; Sun, C.; Duan, Y. Landsat 8 OLI image based terrestrial water extraction from heterogeneous backgrounds using a reflectance homogenization approach. *Remote Sens. Environ.* **2015**, *171*, 14–32. [CrossRef]

60. Maglione, P.; Parente, C.; Vallario, A. Coastline extraction using high resolution WorldView-2 satellite imagery. *Eur. J. Remote Sens.* **2014**, *47*, 685–699. [CrossRef]

61. Kelly, J.T.; Gontz, A.M. Using GPS-surveyed intertidal zones to determine the validity of shorelines automatically mapped by Landsat water indices. *Int. J. Appl. Earth Obs. Geoinf.* **2018**, *65*, 92–104. [CrossRef]

62. Athawuda, A.M.G.A.D.; Jayasiri, H.B.; Thushari, G.G.N.; Guruge, K.P.G.K.P. Quantification and morphological characterization of plastic litter (0.30–100 mm) in surface waters of off Colombo, west coast of Sri Lanka. *Environ. Monit. Assess.* **2020**, *192*, 509. [CrossRef]

63. Perera, K.R.L.; Ranasinghe, D.P.L. An Analysis of Causes of Coastal Erosion in Calido Beach, Kalutara, West Coast of Sri Lanka. *KDU J. Multidiscip. Stud. (KJMS)* **2021**, *3*, 69–79.

64. Lakmali, E.; Deshapriya, W.G.; Ishara Jayawardene, K.G.A.; Raviranga, R.M.; Ratnayake, N.; Premasiri, H.M.; Senanayake, I. Long term coastal erosion and shoreline positions of Sri Lanka. *J. Surv. Fish. Sci.* **2017**, *3*, 69–79. [CrossRef]

65. Warnasuriya, T.W.S.; Gunaalan, K.; Gunasekara, S.S. Google Earth: A New Resource for Shoreline Change Estimation—Case Study from Jaffna Peninsula, Sri Lanka. *Mar. Geod.* **2018**, *41*, 546–580. [CrossRef]

66. Amalan, K.; Ratnayake, A.S.; Ratnayake, N.P.; Weththasinghe, S.M.; Dushyantha, N.; Lakmali, N.; Premasiri, R. Influence of nearshore sediment dynamics on the distribution of heavy mineral placer deposits in Sri Lanka. *Environ. Earth Sci.* **2018**, *77*, 737. [CrossRef]

67. Nijamir, K.; Thennakoon, T.M.S.P.K.; Rupi Herath, H.M.J.; Mohamed Kaleel, M.I. Exploring physical and human induced coastal morphodynamics: A study with reference to nintavur to addalaichenai coastal areas of Ampara District, Sri Lanka. *Acad. J. Interdiscip. Stud.* **2021**, *10*, 347–361. [CrossRef]

68. Ezzeldin, M.M.; Rageh, O.S.; Saad, M.E. Assessment impact of the damietta harbour (egypt) and its deep navigation channel on adjacent shorelines. *J. Integr. Coast. Zone Manag.* **2020**, *20*, 265–281. [CrossRef]

69. Elmoustapha, A.O.; Levoy, F.; Monfort, O.; Koutitonsky, V.G. A numerical forecast of shoreline evolution after harbour construction in Nouakchott, Mauritania. *J. Coast. Res.* **2007**, *23*, 1409–1417. [CrossRef]

70. Dastgheib, A.; Jongejan, R.; Wickramanayake, M.; Ranasinghe, R. Regional scale risk-informed land-use planning using Probabilistic Coastline Recession modelling and economical optimisation: East Coast of Sri Lanka. *J. Mar. Sci. Eng.* **2018**, *6*, 120. [CrossRef]

71. Short, A.D. Macro-meso tidal beach morphodynamics: An overview. *J. Coast. Res.* **1991**, *7*, 417–436.

72. Prasanna, H.M.I.; Gunathilaka, M.D.E.K.; Welikanna, D.R.; Lanka, S. Variability of the Sounding Datums Around Sri Lankan Coastline (10065). In Proceedings of the FIG Working Week, Hanoi, Vietnam, 23–25 April 2019.

73. Frigaard, P.; Margheritini, L. *Oluvil Port Development Project: 3rd Party Opinion on Report by Lanka Hydraulic Institute Ltd.: Oluvil Port Development Project: Studies on Beach Erosion, June 2011*; Aalborg University: Aalborg, Denmark, 2011; Available online: http://vbn.aau.dk/ws/files/58116047/Oluvil_Port_Development_Project_3rd_Party_Opinion_on_Report_by_Lanka_Hydraulic_Institute_Ltd_Oluvil_Port_Development_Project_Studies_on_Beach_Erosion_June_2011.pdf (accessed on 1 December 2022).

74. Wijeratne, E.M.S.; Pattiaratchi, C.B. Sea Level Variability in Sri Lanka Waters. 2003. Available online: http://wcrp.ipsl.jussieu.fr/Workshops/SeaLevel/Posters/2_1_WijeratneRevised.pdf (accessed on 1 December 2022).

75. Zahir, I.L.M.; Madurapperuma, B.; Iyoob, A.L.; Nijamir, K. Exploring the Ever-Changing Seashore Using Geoinformatics Technology. *Earth* **2021**, *2*, 544–555. [CrossRef]

76. Ranasinghe, R.; Duong, T.; Dastgheib, A.; de Boer, W.; de Vroeg, H. *Longshore Sediment Transport (LST) Modelling Study: Trincomalee and Batticaloa Districts (Final Report)*; IHE: Delft, The Netherlands, 2018.

77. Nijamir, K.; Ameer, F.; Thennakoon, S.; Herath, J.; Iyoob, A.L.; Zahir, I.L.M.; Sabaratnam, S.; Fathima Jisna, M.V.; Madurapperuma, B. Geoinformatics application for estimating and forecasting of periodic shoreline changes in the east coast of Ampara District, Sri Lanka. *Ocean Coast. Manag.* **2023**, *232*, 106425. [CrossRef]

78. McFeeters, S.K. Ndwi by Mcfeeters. *Remote Sens. Environ.* **1996**, *25*, 687–711.

79. Oyedotun, T.D.T. Shoreline Geometry: DSAS as a Tool for Historical Trend Analysis. *Geomorphol. Tech.* **2014**, *2*, 1–12.

80. Quang, D.N.; Ngan, V.H.; Tam, H.S.; Viet, N.T.; Tinh, N.X.; Tanaka, H. Long-term shoreline evolution using dsas technique: A case study of Quang Nam province, Vietnam. *J. Mar. Sci. Eng.* **2021**, *9*, 1124. [CrossRef]

81. Velsamy, S.; Balasubramaniyan, G.; Swaminathan, B.; Kesavan, D. Multi-decadal shoreline change analysis in coast of Thiruchendur Taluk, Thoothukudi district, Tamil Nadu, India, using remote sensing and DSAS techniques. *Arab. J. Geosci.* **2020**, *13*, 838. [CrossRef]
82. Sytnik, O.; Del Río, L.; Greggio, N.; Bonetti, J. Historical shoreline trend analysis and drivers of coastal change along the Ravenna coast, NE Adriatic. *Environ. Earth Sci.* **2018**, *77*, 779. [CrossRef]
83. Apostolopoulos, D.N.; Avramidis, P.; Nikolakopoulos, K.G. Estimating Quantitative Morphometric Parameters and Spatiotemporal Evolution of the Prokopos Lagoon Using Remote Sensing Techniques. *J. Mar. Sci. Eng.* **2022**, *10*, 931. [CrossRef]
84. Hewavithana, D.K.; Pieris, A.L.; Peries, T.N.; Wijesinghe, M.R. Discovery of a large nesting colony of the Blue-tailed Bee-eater (Merops philippinus) in Oluvil, Ampara. *Wildlanka* **2017**, *5*, 11–16.
85. Ameer, F. Physical impacts of Oluvil harbour. In Proceedings of the 5th International Symposium, London, UK, 27–28 June 2015; South Eastern University of Sri Lanka: Oluvil, Sri Lanka, 2015.
86. Nijamir, K.; Kaleel, M.I.M. Coastal morphodynamics associated natural hazards: A case study of Oluvil area in Ampara district, Sri Lanka. *World Sci. News* **2018**, *97*, 113–124. Available online: http://yadda.icm.edu.pl/yadda/element/bwmeta1.element.psjd-f043b45b-146d-4bdd-a2c1-831b265dff2d (accessed on 30 November 2022).
87. Almonacid-Caballer, J.; Sánchez-García, E.; Pardo-Pascual, J.E.; Balaguer-Beser, A.A.; Palomar-Vázquez, J. Evaluation of annual mean shoreline position deduced from landsat imagery as a mid-term coastal evolution indicator. *Mar. Geol.* **2016**, *372*, 79–88. [CrossRef]
88. Karaman, M. Comparison of thresholding methods for shoreline extraction from sentinel-2 and landsat-8 imagery: Extreme Lake Salda, track of Mars on Earth. *J. Environ. Manag.* **2021**, *298*, 113481. [CrossRef]
89. Dewidar, K.; Bayoumi, S. Forecasting shoreline changes along the Egyptian Nile Delta Coast using Landsat Image Series and geographic information system. *Environ. Monit. Assess.* **2021**, *193*, 429. [CrossRef] [PubMed]